Versatile Types of DNA-Based Nanobiosensors for Specific Detection of Cancer Biomarker FEN1 in Living Cells and Cell-Free Systems

Hao Zhang,[†,‡] Sai Ba,[†,‡] Divyanshu Mahajan,[§] Jasmine Yiqin Lee,[†] Ruijuan Ye,[†] Fangwei Shao,[†] Lei Lu[,§] and Tianhu Li[*,†]*

†Division of Chemistry and Biological Chemistry, School of Physical and Mathematical Sciences, Nanyang Technological University, Singapore 637371

§School of Biological Sciences, Nanyang Technological University, Singapore 637551

Corresponding Authors:

* Tianhu Li, Ph. D.
Tel: (65) 6513 7364
Fax: (65) 6515 9663
E-mail: thli@ntu.edu.sg

* Lei Lu, Ph. D.
Tel: (65) 6592 2591
Fax: (65) 6791 3856
E-mail: lulei@ntu.edu.sg

ABSTRACT: Flap structure-specific endonuclease 1 (FEN1) is overexpressed in various types of human cancer cells, and has been recognized as a promising biomarker for cancer diagnosis in the recent years. In order to specifically detect the abundance and activity of this cancer-overexpressed enzyme, different types of DNA-based nanodevices were created during our investigations. It is shown in our studies that these newly designed biosensors are highly sensitive and specific for FEN1 in living cells as well as in cell-free systems. It is expected that these nanoprobes could be useful for monitoring FEN1 activity in human cancer cells, and also for cell-based screening of FEN1 inhibitors as new anticancer drugs.

KEYWORDS: Nanodevices; Biosensors; Fluorescent probes; DNA repair enzymes; Graphene oxide

Flap structure-specific endonuclease 1 (FEN1), as one of the most crucial enzymes in eukaryotic cells, catalyzes removal of 5' overhanging DNA flaps in both long-patch DNA base excision repair (BER) pathway and Okazaki fragment maturation during DNA replication.[1-4] Besides playing essential roles in the abovementioned cellular processes, FEN1 has been identified as a reliable biomarker for cancer diagnosis and monitoring over the past few years owing to its overexpression in various types of cancer cells such as testis, lung, breast, prostate and brain cells.[5-8] In addition, since FEN1 was involved in tumor progression and development, and the levels of its expression were correlated to cancer cell survival, proliferation, function and apoptosis, this enzyme has been considered to be a validated therapeutic target of anticancer drugs in the recent years.[9-14] To the best of our knowledge, however, there is no existing diagnostic platform that allows real-time and direct detection of enzymatic activity of FEN1 in live cells. Although some traditional approaches have been developed for detection of other

protein biomarkers, most of these techniques (*e.g.* SDS-PAGE, Western blotting analysis, ELISA-based immunological methods, electrochemical and electrical methods) are limited to fixed cells, cell lysates, or other cell-free systems.[15-17] Even today, the development of precise and real-time diagnostic platforms still faces multiple challenges, which includes (1) poor target accessibility in living cells, (2) relatively low sensitivity and specificity in crowded cellular environments, and (3) low accuracy due to external interferences introduced by the diagnostic methods themselves. Despite the many challenges we are facing, when new biosensors are designed and fabricated, their sensitivity, specificity and accuracy are basic requirements that should be taken into account.

For the current study, in consideration of the facts that (1) FEN1 is well recognized as a cancer biomarker as well as a target of anticancer drugs, and (2) specific biosensors for real-time monitoring of the FEN1 activity of live cells have not yet been developed, we reported here a new series of nanobiosensors based on target-responsive nanocomposites. Our investigations demonstrated that these newly designed nanoprobes are highly sensitive and specific to the level of FEN1 in cell-free systems. In addition, with the help of graphene oxide nanoflakes, the DNA-based probe can readily enter living cells and thus be turned on by the catalytic action of cellular FEN1. Because of the responsive design, these nanobiosensors, different from traditional approaches, can be used for real-time analysis in both living cells and cell-free systems without affecting the activity and abundance of the analyte. Moreover, due to the high turnover number of the target enzyme FEN1, high signal amplification and rapid response times can be easily achieved within cellular environments.

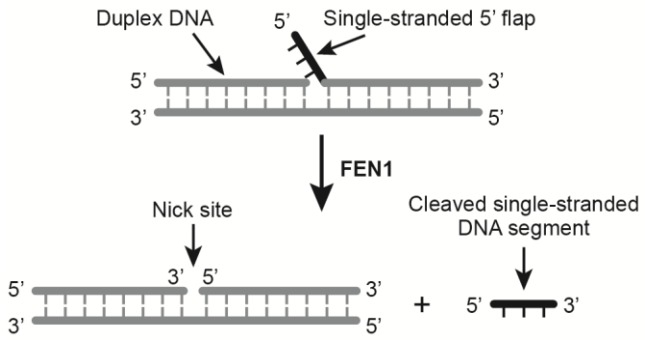

Figure 1. Schematic illustration of catalytic actions of FEN1 on duplex DNA that possesses 5' flap structure.

Over the last few decades, a number of functional nanomaterials with well-controlled size and shape have been created and developed for diagnostic as well as therapeutic applications such as gold nanoparticles, quantum dots and carbon nanotubes.[18-23] Among them, graphene oxide (GO) which is one of the emerging star building materials was used in our studies due to its (1) strong interaction with single-stranded DNA[24-30], (2) distance-dependent fluorescence quenching property[31-36], (3) high water solubility[37, 38], (4) high surface area and high loading capacity[39, 40], (5) robust chemical and mechanical stability[41-43], (6) low cytotoxicity[44, 45] and (7) low-cost and ease of preparation[46, 47]. Furthermore, it has been reported that graphene oxide nanoflakes with certain size are able to pass through cell membrane via endocytosis.[48-50] Based on these biochemical properties of graphene oxide, different types of GO-based nanobiosensors were originally designed and examined in our studies for their susceptibility to FEN1. Figure 2 depicts structures of these five types of DNA-GO nanocomposites (Probe 1 to Probe 5) and their anticipated responses toward catalytic action of FEN1. Each of the five probes is composed of DNA segments and graphene oxide respectively. The DNA segments in these probes on the one hand act as fluorophore carriers, and on the other hand serve as substrates that are responsible for interacting with the target analyte FEN1.[51, 52] Graphene oxide is responsible for transporting

fluorescent FEN1 substrates across cell membranes and causing alteration of fluorescence intensities upon the action of FEN1. Cyanine 3 as a water soluble and pH-insensitive fluorescent dye enables simple and efficient labeling of our DNA structures at various positions.[53, 54]

More specifically, the DNA portion of Probe 1 is a unimolecular dumbbell-shaped structure with a fluorophore (Cy3) at it 5' end and two hairpin loops at both sides of its duplex region. One of the two single-stranded loops in Probe 1 possesses comparatively large size (25 bases), which is specially designed for its adsorption on the surface of graphene oxide. These adsorbing interactions will bring the entire DNA segment close to the surface of graphene oxide, thus leading simultaneously to the quenching of Cy3 fluorescence signals. In addition, as a substrate of the target analyte FEN1, the DNA portion of Probe 1 should be cleavable by the action of FEN1. This will sequentially cause the release of 5' flap and regeneration of fluorescence signal from Probe 1 (Figure 2A).

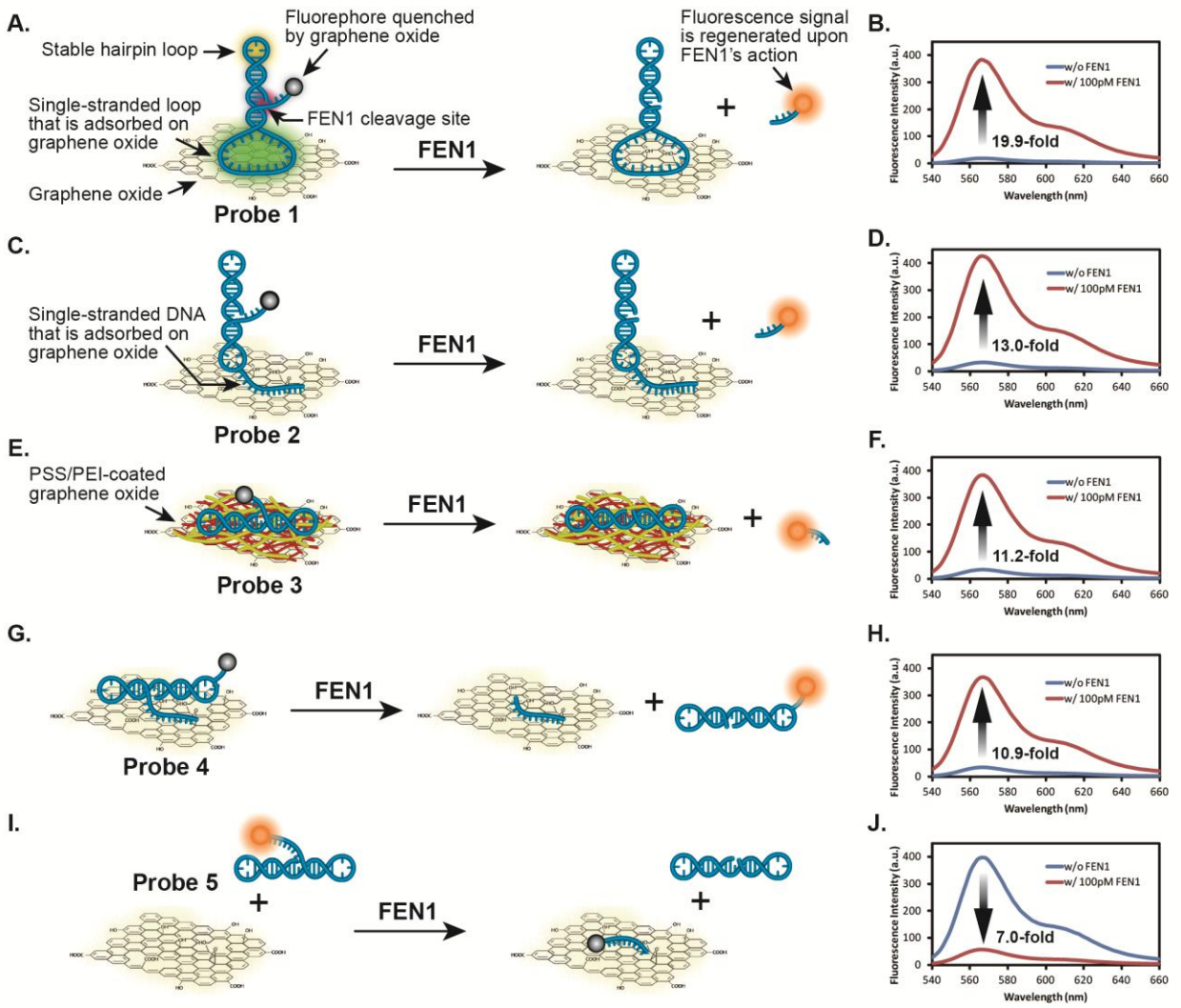

Figure 2. Illustration of structural organizations of our newly designed five DNA-based nanobiosensors (A, C, E, G and I) and their responses to the actions of FEN1 (B, D, F, H and J). Reaction mixtures containing 100 pM of FEN1 and 100 nM of Probe 1 (A and B), Probe 2 (C and D), Probe 3 (E and F), Probe 4 (G and H), Probe 5 (I and J) respectively were incubated in the presence of 50 mM Tris-HCl (pH 7.0), 10 mM $MgCl_2$, 1 mM DTT and 100 μg/ml BSA at 37 °C for 2 hours, followed by fluorescence spectroscopy at an excitation wavelength of 510 nm. Detailed experimental procedures were described in Supporting Information.

Different from Probe 1, the sizes of both loops in Probe 2 are standardized (3-4 bases), to one of which a single stranded DNA segment is covalently linked by click chemistry. Once this single stranded DNA binds to the surface of graphene oxide, fluorescence signals of Cy3 in the hairpin duplex DNA will be quenched by graphene oxide nanosheets and in turn be regenerated by the catalytic action of FEN1 (Figure 2C). Additionally, in contrast to the other four DNA probes shown in Figure 2, poly(sodium 4-styrenesulfonate) (PSS) is adsorbed on the surface of graphene oxide in Probe 3 through non-charged portions of this organic polymer. At the same time, the positively charged side chains of polyethylenimine (PEI) form electrostatic interactions with PSS and thus make the surface-coated graphene oxide polycationic.[55] In this case, the polyanionic duplex DNA entity is able to form electrostatic interactions with PSS/PEI-coated graphene oxide, which will make the sequential quenching and regeneration of Cy3 upon action of FEN1 feasible (Figure 2E). Furthermore, since the 5' flap in FEN1 substrate is a single-stranded overhang, this flap structure is distinctively utilized for its binding interaction with graphene oxide in Probe 4. Unlike the rest of probes shown in Figure 2 where fluorophores are connected to 5' flaps, the Cy3 fluorophore in Probe 4 is covalently linked to the loop region. As a result, upon the action of FEN1, the released product from graphene oxide in Probe 4 will be duplex DNA segments rather than single-stranded flap structures (Figure 2G). Lastly, different from the aforementioned Probes 1-4, fluorescence-labeled DNA segment and graphene oxide in Probe 5 are separate entities instead. It is the adsorption of generated single DNA fragments that leads to variation of fluorescence signals in this probe (Figure 2I).

For the purpose of examining susceptibility of Probe 1 to catalytic action of FEN1 in cell-free systems, Probe 1 and this target enzyme were incubated together in FEN1 reaction buffer during our investigations. As shown in Figure 3A, fluorescence signals were generated from Probe 1 in

the presence of FEN1 whereas their intensities at wavelength of 568 nm increased with the increase of FEN1's concentrations from 0.2 to 100 pM. On the basis of these observations, plots of fluorescence intensity *vs.* FEN1 concentration were graphed accordingly, which revealed that the detection limit (LoD) of FEN1 through using Probe 1 was as low as 0.38 pM (detailed calculation given Supporting Information). In addition, in order to corroborate that activation of Probe 1 is indeed FEN1-specific, a series of DNA-related proteins were examined as well in our studies, which included DNase I, RNase T, DNA ligase 1, topoisomerase I, topoisomerase II, polynucleotide phosphatase/kinase, DNA polymerase β and histones. As seen in Figure 3C, none of these enzymes and proteins was capable of causing evident amount of fluorescence signals from Probe 1. In addition, the responsiveness of Probes 2, 3, 4 and 5 towards the catalytic action of FEN1 were examined as well in our studies. Similar to Probe 1, fluorescence intensities of these four probes varied significantly with the increase of their concentrations (Figures 2D, 2F, 2H and 2J). These results along with the observations shown in Figure 2B indicate that all of our newly designed five graphene oxide-based probes are highly sensitive to catalytic actions of FEN1 in cell-free systems. According to the fluorescence intensity variation of these probes (Figure 2), the order of their detection sensitivity for FEN1 in cell-free systems was as follows: Probe 1 > Probe 2 > Probe 3 > Probe 4 > Probe 5.

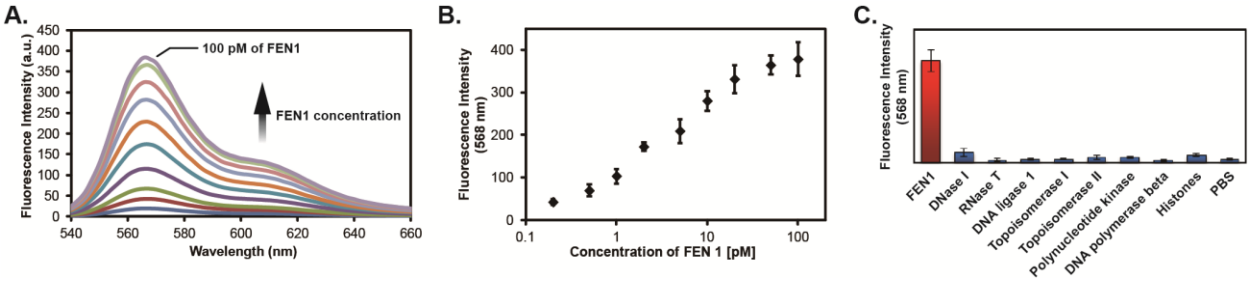

Figure 3. (A) Correlation between fluorescence intensity of Probe 1 and concentration of FEN1. Probe 1 (100 nM) was incubated without FEN1 (blue) or with 0.2 pM (red), 0.5 pM (green), 1

pM (purple), 2 pM (aqua), 5 pM (orange), 10 pM (light blue), 20 pM (light red), 50 pM (light green), 100 pM (light purple) of FEN1 respectively in the presence of 50 mM Tris-HCl (pH 7.0), 10 mM $MgCl_2$, 1 mM DTT and 100 μg/ml BSA at 37 °C for 2 hours, followed by fluorescence spectroscopy at an excitation wavelength of 510 nm. (B) A plot of concentration of FEN1 vs. fluorescence intensity at 568 nm. Calculation of LoD is presented in detail in Supporting Information. (C) Specificity test of Probe 1 towards various DNA-related proteins. Probe 1 (DNA concentration of 100 nM) was incubated with 100 pM of FEN1 (~4 units), DNase I (~0.006 units), RNase T, DNA ligase 1, topoisomerase I, topoisomerase II, polynucleotide phosphatase/kinase, DNA polymerase β, and histones respectively in the presence of 1X FEN1 reaction buffer (50 mM Tris-HCl, 10 mM $MgCl_2$, 1 mM DTT and 100 μg/ml BSA, pH 7.0) at 37 °C for 2 hours, followed by fluorescence examination (emission recorded at 510 nm).

In order to examine response of our newly designed nanoprobes towards its intracellular target FEN1, Probe 1 as the most sensitive one among these five probes was chosen and examined in our next investigations. In addition, since overexpression of FEN1 has been reported in various types of cancer cells,[5-8] a human breast cancer cell line MCF-7, was tested as a representative example of such cancer cells in our studies. MCF-7 cells were accordingly cultured followed by treatment with Probe 1 and inhibitors of FEN1. As shown in Figure 4, in the presence of FEN1 inhibitors aurintricarboxylic acid (ATA, Row B) and NSC-13755 (NSC, Row C), the Cy3 fluorescence signal in MCF-7 cell images was found to be nearly negligible. This happened because catalytic activity of FEN1 in MCF-7 cells was suppressed by ATA and NSC-13755,[52, 56] which lacked the ability to remove fluorescent 5' flap from Probe 1 any longer. On the other hand, the absence of Cy3 signals in MCF-7 cells can also be taken as an indicative that Probe 1 is not responsive to other enzymes that are present in MCF-7 cells. When cells were incubated with

Probe 1 in the absence of FEN1 inhibitors, fluorescence signals of Cy3 manifested significantly (Row A in Figure 4). This manifestation suggests that (1) graphene oxide was able to effectively transport fluorescent duplex DNA segments across cell membranes, and (2) the duplex DNA segments on graphene oxide was able to act as substrates of cellular FEN1. In a brief summary, the observations shown in Figure 4 demonstrate that our newly designed Probe 1 might be a useful tool for distinguishing the living cells that possess abundantly active FEN1 (Figure 4A) from those that hold low activity of FEN1 (Figures 4B and 4C).

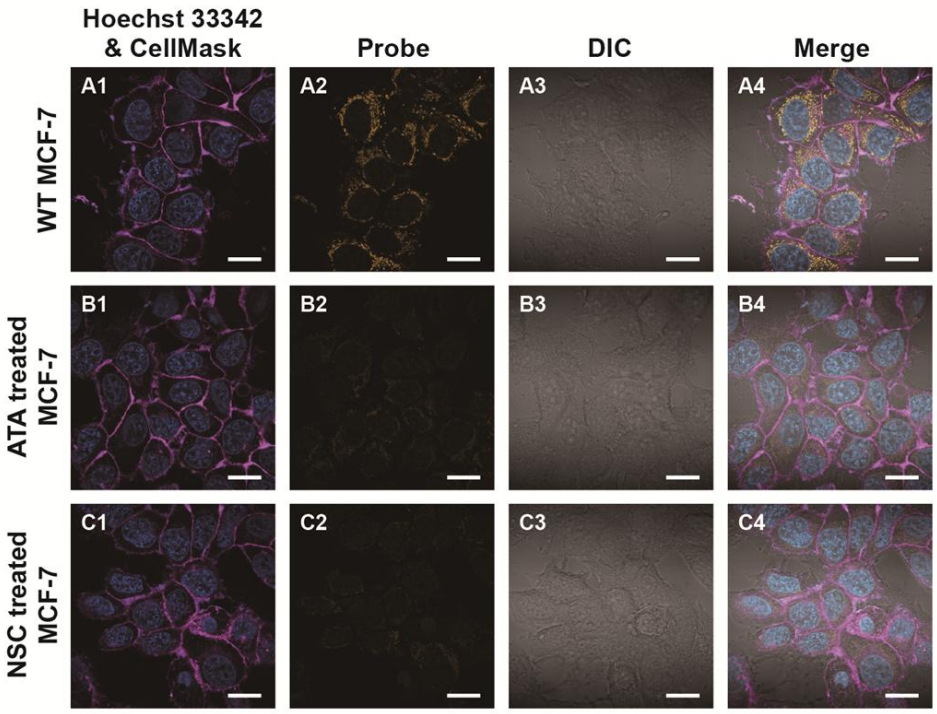

Figure 4. Confocal fluorescence microscopy images of differently treated MCF-7 cells. Cells that were pre-treated without (Row A) or with 1 μM of FEN1 inhibitor ATA (Row B) or NSC-13755 (Row C) for 2 hours and then incubated with Probe 1 at 37 °C for 4 hours. Cell membranes were stained with CellMask™ Plasma membrane Stain (purple) while nuclei were stained with Hoechst 33342 (blue). Light transmission images (DIC) displayed the morphology

of the cells. Merged images showed the overlay of four channels (CellMask, Hoechst 33342, Cy3 and DIC). Scale bars represent 20 μm.

Three different-sized graphene oxide nanosheets (Figure 5A) were prepared next in our studies in order to find out how dimensions of these nanosheets affect their uptake efficiency by MCF-7 cells. Our confocal examination showed that the graphene oxide with its lateral size of ~0.1 μm displayed highest efficiency when they are passing across plasma membranes of the cells (Figure 5B). In addition, time dependence of cellular uptake of Probe 1 was examined in our studies. As shown in Figure S1, significant amount of fluorescence signals emerged after incubation of Probe 1 with MCF-7 cells for 1.5 and 4 hours, which reflects the time periods needed for graphene oxide to pass across plasma membranes and for FEN1 to remove 5' flaps from its DNA substrates. Moreover, an MTT-based cell viability assay was carried out to evaluate the cytotoxic effect of these DNA-based nanobiosensors. The results shown in Figure S2 demonstrated that no significant cytotoxic effect was observed in cells incubated with any of the five probes.

Besides the aforementioned studies that were carried out in living cells, a series of experiments were conducted in cell-free systems during our investigations. Probe 1 was incubated with or without FEN1 in the buffer solution followed by exposure under UV light with the wavelength of 302 nm. As seen in Figure S3, these FEN1 reaction products monitored by fluorescence emission displayed much more intensive color than Probe 1 alone, which implies that Probe 1 could be used conveniently for *in vitro* screening FEN1 inhibitors from libraries of synthetic and natural products. With the aim of confirming that fluorescence signals were indeed produced by the action of FEN1, the DNA portion of Probe 1 alone was examined by gel electrophoresis. As seen in Figure S4, the reaction products migrated faster than the original DNA portion of Probe 1, which signifies that lower molecular weight products were formed upon the action of FEN1. In

addition, morphology of the DNA-GO nanocomposites was characterized by AFM and TEM (Figure S5) in order to verify that fluorophore-labeled oligonucleotides were indeed adsorbed onto the surface of graphene oxide.

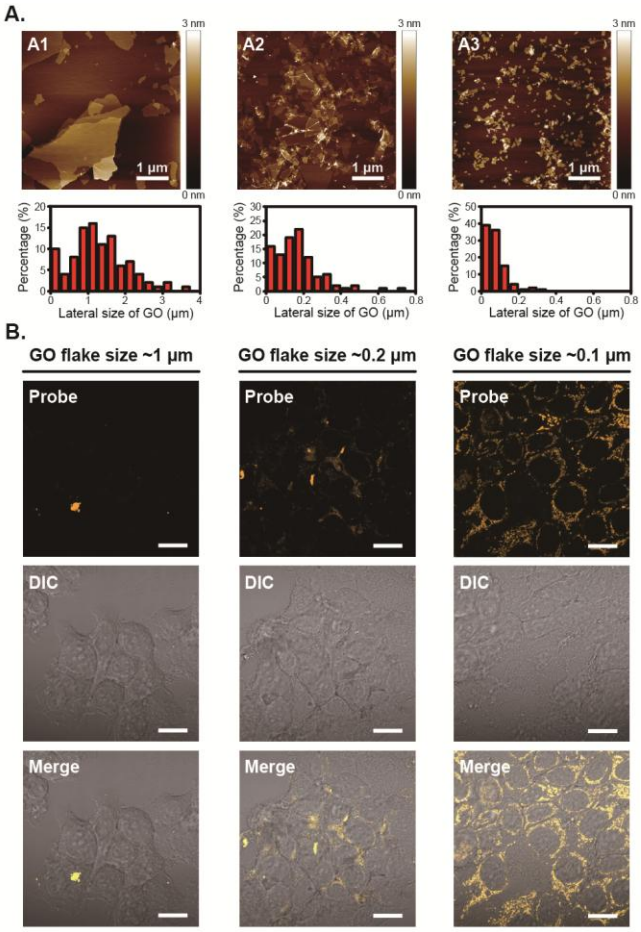

Figure 5. (A) AFM images of different-sized graphene oxide nanosheets and distributions of their lateral size. The AFM images in A1, A2 and A3 are corresponding graphene oxide nanosheets with lateral sizes of ~1 μm, ~0.2 μm and ~0.1 μm respectively. (B) Cellular uptake efficiency of three different-sized graphene oxide nanosheets by MCF-7 cells. Scale bars represent 20 μm.

In conclusion, five different types of nanodevices were created and examined during our investigations, which consist of graphene oxide nanosheets and fluorophore-containing DNA

respectively. Since these newly designed FEN1 turn-on fluorescent probes could be used to detect a limited amount of cells and are highly responsive to cancer-overexpressed FEN1, they could be further developed as a general approach for noninvasive cancer diagnosis, and could benefit the discovery of future generations of anticancer drugs.

AUTHOR INFORMATION

Corresponding Authors
*thli@ntu.edu.sg
*lulei@ntu.edu.sg

Author Contributions
‡These authors contributed equally to this work.

ACKNOWLEDGMENT

This work was supported by Ministry of Education in Singapore and Nanyang Technological University through research Grants (MOE2014-T2-2-042, MOE RG14/15, MOE RG13/16 and MOE RG117/17) to Tianhu Li.

SUPPORTING INFORMATION

The Supporting Information is available free of charge on the ACS Publications website at…

Materials, detailed experimental procedures and supporting figures (PDF)

REFERENCES

(1) Bambara, R. A.; Murante, R. S.; Henricksen, L. A. *Journal of Biological Chemistry* **1997,** *272*, 4647-4650.

(2) Burgers, P. M. J. *Journal of Biological Chemistry* **2009,** *284*, 4041-4045.

(3) Tsutakawa, S. E.; Classen, S.; Chapados, B. R.; Arvai, A. S.; Finger, L. D.; Guenther, G.; Tomlinson, C. G.; Thompson, P.; Sarker, A. H.; Shen, B. H.; Cooper, P. K.; Grasby, J. A.; Tainer, J. A. *Cell* **2011,** *145*, 198-211.

(4) Finger, L. D.; Atack, J. M.; Tsutakawa, S.; Classen, S.; Tainer, J.; Grasby, J.; Shen, B. *Sub-cellular biochemistry* **2012,** *62*, 301-26.

(5) Nikolova, T.; Christmann, M.; Kaina, B. *Anticancer research* **2009,** *29*, 2453-2459.

(6) He, L. F.; Zhang, Y. L.; Sun, H. F.; Jiang, F.; Yang, H.; Wu, H.; Zhou, T.; Hu, S. C.; Kathera, C. S.; Wang, X. J.; Chen, H. Y.; Li, H. Z.; Shen, B. H.; Zhu, Y. Q.; Guo, Z. G. *Ebiomedicine* **2016,** *14*, 32-43.

(7) Lam, J. S.; Seligson, D. B.; Yu, H.; Li, A.; Eeva, M.; Pantuck, A. J.; Zeng, G.; Horvath, S.; Belldegrun, A. S. *Bju Int* **2006,** *98*, 445-451.

(8) Abdel-Fatah, T. M. A.; Russell, R.; Albarakati, N.; Maloney, D. J.; Dorjsuren, D.; Rueda, O. M.; Moseley, P.; Mohand, V.; Sun, H. M.; Abbotts, R.; Mukherjee, A.; Agarwal, D.; Illuzzi, J. L.; Jadhave, A.; Simeonov, A.; Ball, G.; Chan, S.; Caldas, C.; Ellis, I. O.; Wilson, D. M.; Madhusudan, S. *Molecular oncology* **2014,** *8*, 1326-1338.

(9) Doherty, R.; Madhusudan, S. *J Biomol Screen* **2015,** *20*, 829-841.

(10) Kathera, C.; Zhang, J.; Janardhan, A.; Sun, H. F.; Ali, W.; Zhou, X. L.; He, L. F.; Guo, Z. G. *Oncotarget* **2017,** *8*, 27593-27602.

(11) Zheng, L.; Jia, J.; Finger, L. D.; Guo, Z. G.; Zer, C.; Shen, B. H. *Nucleic Acids Res* **2011,** *39*, 781-794.

(12) He, L. F.; Luo, L. B.; Zhu, H.; Yang, H.; Zhang, Y. L.; Wu, H.; Sun, H. F.; Jiang, F.; Kathera, C. S.; Liu, L. J.; Zhuang, Z. H.; Chen, H. Y.; Pan, F. Y.; Hu, Z. G.; Zhang, J.; Guo, Z. G. *Molecular oncology* **2017,** *11*, 640-654.

(13) Zhang, K. Q.; Keymeulen, S.; Nelson, R.; Tong, T. R.; Yuan, Y. C.; Yun, X. W.; Liu, Z.; Lopez, J.; Raz, D. J.; Kim, J. Y. *Am J Pathol* **2018,** *188*, 242-251.

(14) Xie, C. H.; Wang, K. J.; Chen, D. R. *Molecular medicine reports* **2016,** *13*, 386-392.

(15) Wu, L.; Qu, X. *Chemical Society reviews* **2015,** *44*, 2963-97.

(16) Osborne, C.; Brooks, S. A. *Methods in molecular medicine* **2006,** *120*, 217-29.

(17) Pumera, M.; Ambrosi, A.; Bonanni, A.; Chng, E. L. K.; Poh, H. L. *Trac-Trend Anal Chem* **2010,** *29*, 954-965.

(18) Rosi, N. L.; Mirkin, C. A. *Chemical reviews* **2005,** *105*, 1547-1562.

(19) Cao, Y. C. *Nanomedicine* **2008,** *3*, 467-469.

(20) Song, S. P.; Qin, Y.; He, Y.; Huang, Q.; Fan, C. H.; Chen, H. Y. *Chemical Society reviews* **2010,** *39*, 4234-4243.

(21) Ji, T. J.; Zhao, Y.; Ding, Y. P.; Nie, G. J. *Advanced materials* **2013,** *25*, 3508-3525.

(22) Holzinger, M.; Le Goff, A.; Cosnier, S. *Front Chem* **2014,** *2*.

(23) Chen, G. Y.; Roy, I.; Yang, C. H.; Prasad, P. N. *Chemical reviews* **2016,** *116*, 2826-2885.

(24) Li, F.; Liu, X.; Zhao, B.; Yan, J.; Li, Q.; Aldalbahi, A.; Shi, J.; Song, S.; Fan, C.; Wang, L. *ACS applied materials & interfaces* **2017,** *9*, 15245-15253.

(25) He, S.; Song, B.; Li, D.; Zhu, C.; Qi, W.; Wen, Y.; Wang, L.; Song, S.; Fang, H.; Fan, C. *Adv Funct Mater* **2010,** *20*, 453-459.

(26) Liu, B. W.; Sun, Z. Y.; Zhang, X.; Liu, J. W. *Analytical chemistry* **2013,** *85*, 7987-7993.

(27) Wu, M.; Kempaiah, R.; Huang, P. J. J.; Maheshwari, V.; Liu, J. W. *Langmuir* **2011,** *27*, 2731-2738.

(28) Wang, Y.; Tang, L. H.; Li, Z. H.; Lin, Y. H.; Li, J. H. *Nature protocols* **2014,** *9*, 1944-1955.

(29) Manohar, S.; Mantz, A. R.; Bancroft, K. E.; Hui, C. Y.; Jagota, A.; Vezenov, D. V. *Nano letters* **2008,** *8*, 4365-4372.

(30) Varghese, N.; Mogera, U.; Govindaraj, A.; Das, A.; Maiti, P. K.; Sood, A. K.; Rao, C. N. R. *Chemphyschem : a European journal of chemical physics and physical chemistry* **2009,** *10*, 206-210.

(31) Li, F.; Pei, H.; Wang, L.; Lu, J.; Gao, J.; Jiang, B.; Zhao, X.; Fan, C. *Adv Funct Mater* **2013,** *23*, 4140-4148.

(32) Zhu, Y. W.; Murali, S.; Cai, W. W.; Li, X. S.; Suk, J. W.; Potts, J. R.; Ruoff, R. S. *Advanced materials* **2010,** *22*, 3906-3924.

(33) Pumera, M. *Mater Today* **2011,** *14*, 308-315.

(34) Chen, D.; Feng, H. B.; Li, J. H. *Chemical reviews* **2012,** *112*, 6027-6053.

(35) Hong, G. S.; Diao, S. O.; Antaris, A. L.; Dai, H. J. *Chemical reviews* **2015,** *115*, 10816-10906.

(36) Liu, J. H.; Wang, C. Y.; Jiang, Y.; Hu, Y. P.; Li, J. S.; Yang, S.; Li, Y. H.; Yang, R. H.; Tan, W. H.; Huang, C. Z. *Analytical chemistry* **2013,** *85*, 1424-1430.

(37) Si, Y.; Samulski, E. T. *Nano letters* **2008,** *8*, 1679-1682.

(38) Neklyudov, V. V.; Khafizov, N. R.; Sedov, I. A.; Dimiev, A. M. *Physical Chemistry Chemical Physics* **2017,** *19*, 17000-17008.

(39) Montes-Navajas, P.; Asenjo, N. G.; Santamaría, R.; Menéndez, R.; Corma, A.; García, H. *Langmuir* **2013,** *29*, 13443-13448.

(40) Kim, F.; Cote, L. J.; Huang, J. *Advanced materials* **2010,** *22*, 1954-1958.

(41) Suk, J. W.; Piner, R. D.; An, J.; Ruoff, R. S. *Acs Nano* **2010,** *4*, 6557-6564.

(42) Chowdhury, I.; Duch, M. C.; Mansukhani, N. D.; Hersam, M. C.; Bouchard, D. *Environmental science & technology* **2013,** *47*, 6288-6296.

(43) Eigler, S.; Grimm, S.; Hof, F.; Hirsch, A. *J Mater Chem A* **2013,** *1*, 11559-11562.

(44) Liao, K.-H.; Lin, Y.-S.; Macosko, C. W.; Haynes, C. L. *ACS applied materials & interfaces* **2011,** *3*, 2607-2615.

(45) Horvath, L.; Magrez, A.; Burghard, M.; Kern, K.; Forro, L.; Schwaller, B. *Carbon* **2013,** *64*, 45-60.

(46) Chen, J.; Yao, B.; Li, C.; Shi, G. *Carbon* **2013,** *64*, 225-229.

(47) Ranjan, P.; Agrawal, S.; Sinha, A.; Rao, T. R.; Balakrishnan, J.; Thakur, A. D. *Sci Rep-Uk* **2018,** *8*, 12007.

(48) Yang, Y. Q.; Asiri, A. M.; Tang, Z. W.; Du, D.; Lin, Y. H. *Mater Today* **2013,** *16*, 365-373.

(49) Wu, S. Y.; An, S. S. A.; Hulme, J. *International journal of nanomedicine* **2015,** *10*, 9-24.

(50) Zhang, B.; Wei, P.; Zhou, Z. X.; Wei, T. T. *Advanced drug delivery reviews* **2016,** *105*, 145-162.

(51) van Pel, D. M.; Barrett, I. J.; Shimizu, Y.; Sajesh, B. V.; Guppy, B. J.; Pfeifer, T.; McManus, K. J.; Hieter, P. *PLoS genetics* **2013,** *9*.

(52) Dorjsuren, D.; Kim, D.; Maloney, D. J.; Wilson, D. M.; Simeonov, A. *Nucleic Acids Res* **2011,** *39*.

(53) Boutorine, A. S.; Novopashina, D. S.; Krasheninina, O. A.; Nozeret, K.; Venyaminova, A. G. *Molecules* **2013,** *18*, 15357-15397.

(54) Fegan, A.; Shirude, P. S.; Balasubramanian, S. *Chemical communications (Cambridge, England)* **2008**, 2004-2006.

(55) Zhi, F.; Dong, H. F.; Jia, X. F.; Guo, W. J.; Lu, H. T.; Yang, Y. L.; Ju, H. X.; Zhang, X. J.; Hu, Y. Q. *PloS one* **2013,** *8*.

(56) Deshmukh, A. L.; Chandra, S.; Singh, D. K.; Siddiqi, M. I.; Banerjee, D. *Molecular bioSystems* **2017,** *13*, 1630-1639.

TABLE OF CONTENTS GRAPHIC

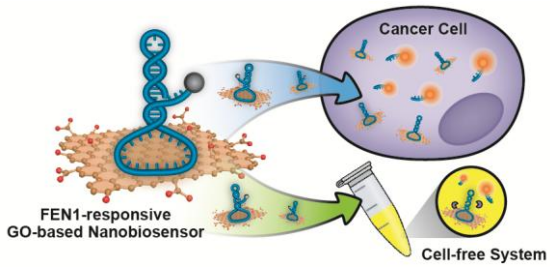

(for TOC only)